X-Ray Attenuation Modeling

Prepared by Incom Inc

Updated February 3rd, 2009

1. Introduction

Incom fiber optic faceplates are used in a variety of medical diagnostic x-ray applications such as digital radiography (intra-oral faceplates, panoramic faceplates and larger area faceplates). In most cases, a fiber optic faceplate of a few millimeters thickness is placed between a thin scintillator layer and a CCD or CMOS sensor. The function of the faceplate is to transmit visible light from scintillator to the detector and block as much x-ray as possible to protect the CCD or CMOS sensor. Incom's faceplates not only protect the sensors from harmful x-rays they also improve image quality.

The objective of this project is to provide technical knowledge on x-ray attenuation of Incom faceplates. Tools such as charts, plots and numerical data will assist Incom in marketing its products, as well as addressing customer questions and concerns. This internal report is aimed to capture all related background and each step in the development of x-ray attenuation modeling for future reference.

The products under discussion are B7D59-6, B7D61-6, BIE395-6, BXE387-6 these four materials represent Incom's X-Ray blocking product line. All four types have a statistical EMA configuration. The x-ray attenuation of each product will be addressed.

2. X-Ray interaction with materials

2.1 X-ray energy level

The quantum energy of electromagnetic spectrum stretches from 10^{-9} eV of low frequency AM radio wave to more than 10 MeV of gamma ray. Different parts of the spectrum have very different effects upon interaction with matter. X-ray usually accounts for a wavelength range from 10^{-8} m to 10^{-12} m, i.e. 124 eV to 1.24 MeV in terms of photon energy.

X-ray energy on the order of 1 MeV has been used for radiation therapy and energy range from 0.02 MeV to 0.1 MeV has been widely applied to diagnostic imaging. Since different customers may design their products to target different imaging applications, the final energy of x-ray that Incom products interact with needs to be confirmed by Incom's customers. According to Wang and Blackburn's statistics[1], spectral distribution of imaging x-ray radiation transmitted through patient peaks at 0.05 MeV as shown in Figure 1.

2.2 Interaction of x-ray with materials

Since x-ray photon energies are above the ionization/excitation/binding energies of atoms, all x-rays are classified as ionizing radiation. When x-ray passes through a patient, the major interactions occur either by giving all of the x-ray energy to an electron to help it eject from the atom (photoelectric ionization or absorption) or by giving part of the energy to the electron and the reminder to a lower energy x-ray photon (Compton scattering). In some scattering, the x-ray is initially absorbed by the atom, but is rapidly re-emitted in an arbitrary direction with unchanged photon energy (coherent scattering). The relative probability of the three types of interactions is material dependent. At sufficiently high energies, i.e. > 1.02 MeV, electron-positron pair production becomes the dominant mode for the interaction of x-rays and gamma rays with matter. Figure 2 illustrated the process of photoelectric absorption, coherent scattering and Compton scattering.

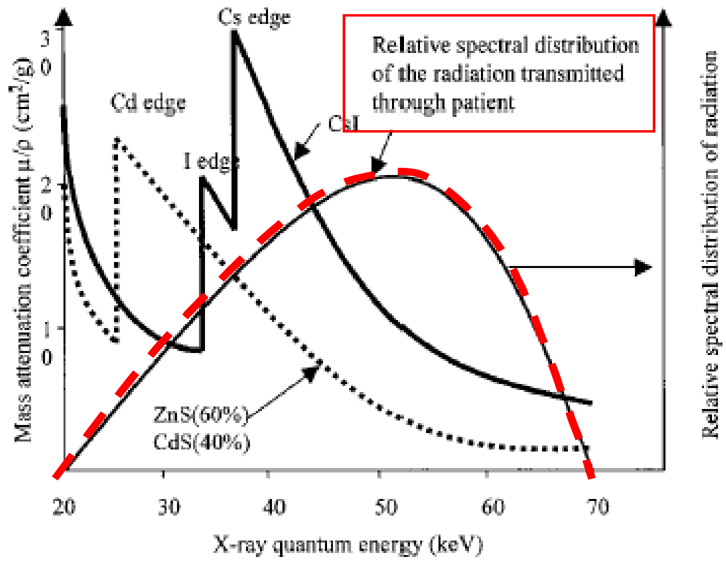

Figure 1 - The relative distribution of radiation through patient is plotted as a function of x-ray photon energy (red-highlighted line).

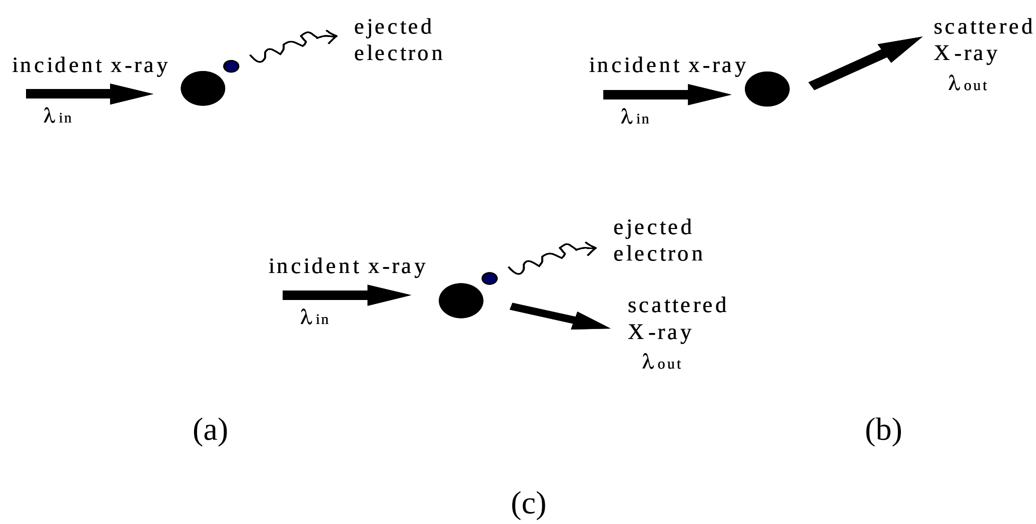

Figure 2 - illustrated the process of photoelectric absorption, coherent scattering and Compton scattering.

Photoelectric absorption,
also known as photoelectric effect or photo-ionization, is a process in which a x-ray photon impinging on an atom transfers its entire energy to an inner shell (e.g. K shell) electron of the atom. The electron (named photoelectron) is ejected/excited/ionized from the atom. The kinetic energy of the ejected photoelectron is equal to the incident x-ray photon energy minus the binding energy of the electron. The vacancy resulting from the ejection is filled by an electron from an outer orbit (e.g. L shell) with lower binding energy, leaving a vacancy in this outer orbit, which in turn is filled by another electron from an orbit even further away (e.g. M shell) from the nucleus. The surplus energy liberated when an electron drops from its outer shell to a shell closer to the nucleus results in emission of characteristic radiation (e.g. Kα line). The energy of the characteristic radiation is equal to the difference in binding energies between shells. Figure 3 (a) depicts a simplified atomic structure with ejected electron under x-ray excitation. The corresponding energy level diagram of an atom is shown in Figure 3 (b), illustrated the excitation of K, L, M and N shells and the formation of Kα, Kβ, Lα and Mα emissions.

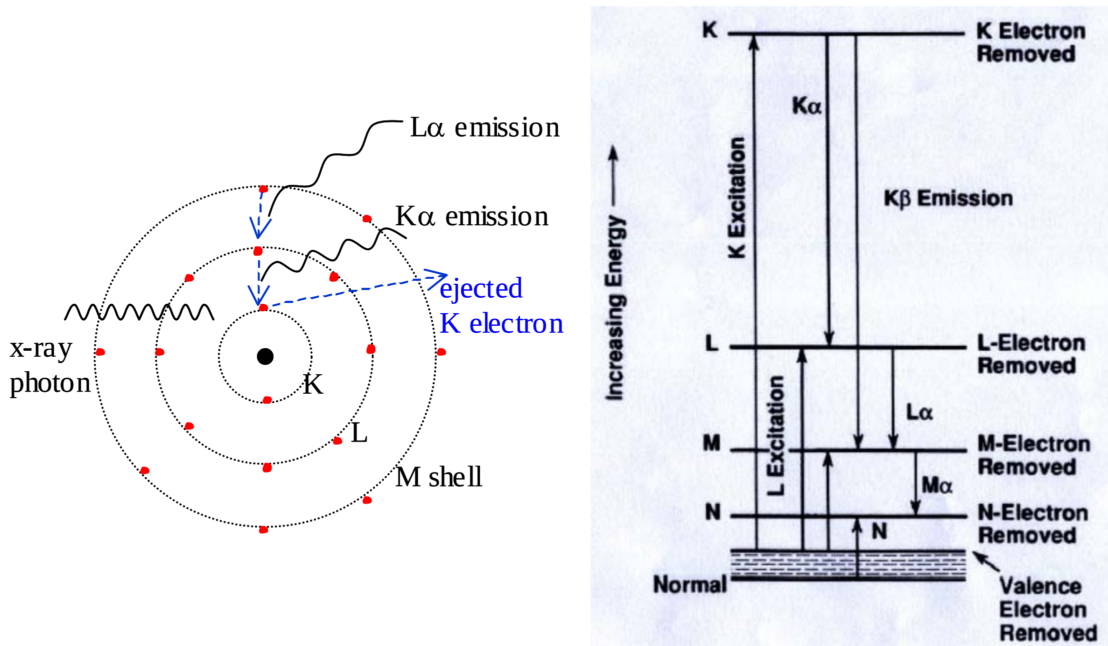

(a) (b)

Figure 3 - (a) Atomic shell structure with ejection of inner shell electron under x-ray radiation. (b) The energy level diagram of an atom, illustrating the excitation of K, L, M and N shells and the formation of Kα, Kβ, Lα and Mα radiations.

The binding energy of a K-electron increases with increasing atomic number. It is only 14 eV in the lightest element hydrogen, but increases to 88 keV in lead. The probability of photoelectric absorption per unit mass of a material is approximately proportional to Z^3/E^3, where Z is the atomic number of the material and E is the energy of the incident photon. Photoelectric absorption therefore increases with increasing atomic number and decreasing x-ray photon energy.

It explains the large differences in attenuation between water (soft tissue), bone and lead. The linear attenuation coefficient for these substances at 0.03 MeV are 0.036, 0.16, and 33 mm^{-1}, respectively, resulting in a 50% attenuation thickness of 19, 4.3, and only 0.02 mm[2].

The chance of photoelectric interaction falls steeply and continuously with increasing photon energy, but at absorption edges (K edge, L edge, etc.) it suddenly increases due to photoelectric absorption of the photons.

Coherent scattering,
also known as Rayleigh scattering, is an elastic process where a photon impinging on an atom is scattered without loosing any of its energy. The energy of x-ray photon is first completely absorbed and then re-emitted by electrons of an atom. The scattered photon has the same phase as the incident photon due to unchanged frequency and wavelength ($\lambda out = \lambda in$), however the direction of re-emission is totally arbitrary. The probability of this process increases with decreasing energy of the photons and increasing atomic number of the scattering atom.

Compton scattering,
also known as incoherent scattering, can be considered as a collision between x-ray photon and one of the outer shell electrons of an atom. The outer shell electron is bound with very little energy to the atom and is easy to be ionized. The kinetic energy to help electron’s ejection from the atom is transferred from the incident photon, leaving the scattered x-ray with less photon energy ($Eout < Ein$) and longer wavelength ($\lambda out > \lambda in$). The probability of this process falls gradually with energy of the photons and independent of atomic number of material.

Because energy and momentum are both conserved in this collision, the energy and direction of the scattered x-ray photon depend on the energy transferred to the electron. When the incident x-ray energy is high, the relative amount of energy lost to the electron is small, and the scattering angle is small relative to the initial direction. When the incident x-ray energy is small, the scattering is more isotropic in all directions. At x-ray energies on the order of 1 MeV, the scattering is mostly in the forward direction. At x-ray energies of near 0.1 MeV, the scattering is more isotropic.

3. Data collection and attenuation modeling

The material attenuation of diagnostic imaging x-ray, ranging from 0.02 MeV to 0.1 MeV, mainly comes from photoelectric absorption and Compton scattering mechanism, with incoherent scattering only contributing to a small fraction of total attenuation. All attenuation data used in this report is downloaded from NIST database at http://physics.nist.gov .

3.1 NIST database and assumption

A narrow beam of mono-energetic photons with an incident intensity I_{in}, penetrating a layer of material with thickness t and density ρ, emerges with intensity I_{out} given by the exponential attenuation law

$$\frac{I_{out}}{I_{in}} = e^{-(\mu/\rho)\cdot\rho\cdot t} \qquad \text{(Eq 1)}$$

where μ/ρ (cm^2/g) is mass attenuation coefficient, defined as the linear attenuation coefficient μ (cm^{-1}) divided by the density of the medium. For a given incident x-ray energy, the mass attenuation coefficient is independent of the physical and chemical state of the absorber. Thus, the mass attenuation coefficient is the same for water whether present in liquid or vapor form.

The attenuation of x-ray by certain material depends on the energy of x-ray photon and the following material parameters: thickness, density and atomic number. The mass attenuation coefficients in NIST database cover elements from hydrogen to uranium (Z = 1 ~ 92) and energy grid from 0.1 MeV to 20 MeV, with photoelectric absorption edges (K, L, etc.) being identified. Values of μ/ρ are given just above and below each edge to facilitate accurate interpolation. Figure 4 is the mass attenuation curve of lead (Pb) element plotted in logarithmic scale based on database value with its absorption edge marked.

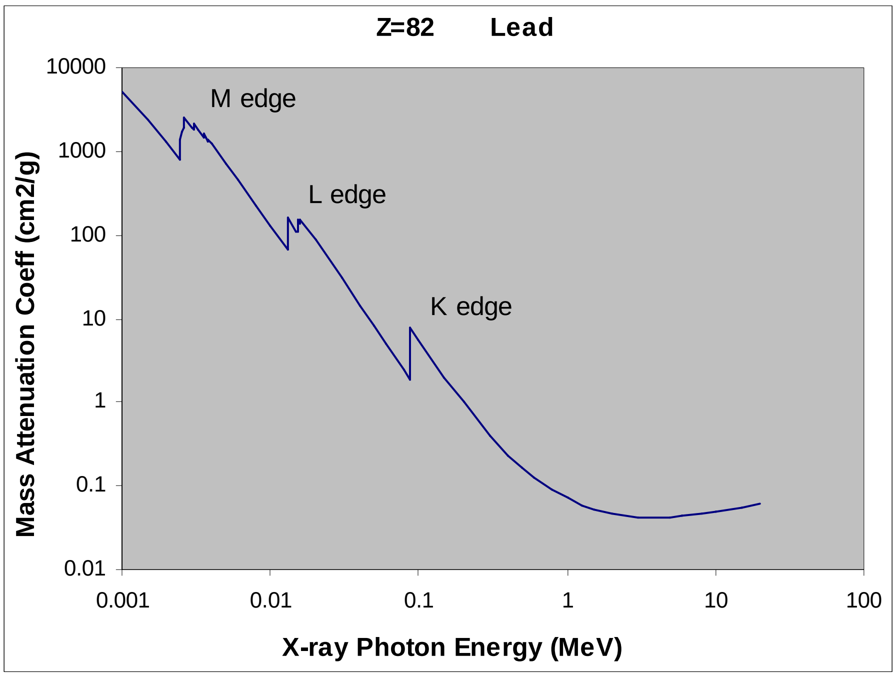

Figure 4 - Mass attenuation coefficient of lead (Pb) versus photon energy.

The μ/ρ provided in NIST database rely heavily on theoretical values of the total attenuation cross section per atom, σ_{tot}, which is related to μ/ρ according to

$$\mu/\rho = \sigma_{tot} \;/\; u \cdot A \qquad \text{(Eq 2)}$$

where u is the atomic mass unit ($u = 1.66 \times 10^{-24}$ g) and A is the relative atomic mass of the target element. σ_{tot} is the total cross section for an interaction by the photon, frequently given in units of b/atom (barns/atom), where b = 10^{-24} cm^2.

The attenuation coefficient, photon interaction cross section and related quantities are functions of the photon energy. Explicit indication of this functional dependence has been omitted to improve readability. The total cross section can be written as the sum over contributions from the principal photon interactions,

$$\mu/\rho = (\sigma_{pe} + \sigma_{coh} + \sigma_{comp} + \sigma_{pair} + \sigma_{trip}) / u{\cdot}A \qquad \text{(Eq 3)}$$

where σ_{pe} is the photoelectric absorption cross section, σ_{coh} and σ_{comp} are the coherent (Rayleigh) and the incoherent (Compton) scattering cross sections, respectively, σ_{pair} and σ_{trip} are the cross sections for electron-positron pairs (e-, e+) production in the fields of the atomic nucleus and electron-positron triplets (2e-, e+) production in the fields of the atomic electrons, respectively.

The NIST mass attenuation coefficient is calculated based on following assumptions.
Assumption 1: Total cross section (σ_{tot}).

Photonuclear absorption ($\sigma_{ph.n}$) of the photon by the atomic nucleus results most usually in the ejection of one or more neutrons and/or protons. This interaction can contribute as much as 5 % to 10 % to the total photon interaction cross section in a fairly narrow energy region usually between 5 MeV and 40 MeV, depending on where the giant resonance of the target nuclide falls. This cross section has not been included in the total cross section calculation due to several difficulties including an irregular dependence on both Z and A and lack of theoretical models. Also, other less-probable photon-atom interactions, such as nuclear-resonance scattering and Delbrück scattering are also omitted.

Assumption 2: Absorption edge.

As explained in Photoelectric Absorption, absorption edge corresponds to the ionization energy of inner shell electron (K, L, M …). It indicates the increased probability of photoelectric absorption that drops sharply as the difference between the incident photon energy and electron binding energy increases. The fine structure of absorption edge is ignored in the calculation because it varies with chemical composition, phase and temperature of compounds. Therefore the calculated attenuation value at photon energy levels near absorption edges is only estimation and should be examined by measurement. The cross sections in the vicinity of absorption edges are assumed to have simple saw-tooth shapes. Values at edges have been obtained by extrapolation of the near-edge sub-shell cross sections to the threshold edge energies.

Assumption 3: Homogenous mixture.

After the theoretical calculation of mass attenuation coefficient of each element, a simple additivity is applied to compounds assumed homogenous mixture by

$$\mu/\rho = \sum_i w_i (\mu / \rho)_i \qquad \text{(Eq 4)}$$

where w_i is the weight fraction of the ith atomic constituent.

3.2 Modeling

Incom has several types of fiber optic faceplate products targeted at medical and dental imaging applications. In order to better market products, a detailed and accurate theoretical model addressing x-ray attenuation versus faceplate thickness versus x-ray photon energy is critical. For example, some customers would like to know the level of attenuation that can be achieved for faceplates of various thicknesses. Others may want to know what thickness sufficiently attenuates 99% to 99.9% of incident x-ray photon to achieve long lifetime of CCD and Complementary metal–oxide–semiconductor (CMOS) detectors, while keeping the smallest dimension of their devices. The model described here will answer this kind of question.

Two of Incom's faceplates, B7D59-6, B7D61-6, which are made from same core (X26), clad (C5) and EMA (B7) materials will be used as examples to demonstrate the process used for determining x-ray attenuation. X-ray attenuation data for the components of BIE395-6 and BXE387-6 material can be found in the appendix. First, the mass attenuation coefficients (μ/ρ) of core, clad and EMA at different x-ray energies can be calculated through a simple additivity of weight fractional contribution from each element presented in raw materials. Then area average is taken according to the area fraction of core, clad and EMA in cross section of each product.

Step 1. Transfer chemical composition of raw materials (X26, C5, B7) into weight fractions of constituent elements.
Step 2. Download mass attenuation coefficient (μ/ρ) of all elements from NIST database.
Step 3. Calculate μ/ρ curves of X26, C5, B7 respectively according to (eq 4).
Step 4. Calculate area fraction of core, clad and EMA for different products based on different core/clad ratio and EMA configurations.
Step 5. Area averaged mass attenuation coefficient = X26 coefficient * core fraction + C5 coefficient * clad fraction + B7 coefficient * EMA fraction.
Step 6. Plot averaged mass attenuation curve versus incident photon energy.

With averaged mass attenuation curve plotted for each product, the faceplate thickness to achieve 99% or 99.9% x-ray attenuation at certain photon energy level can be easily derived from (Eq 1). For 1% transmission (i.e. 99% attenuation), the thickness *t* in millimeter can be expressed as

$$t = \frac{46.05}{(\mu/\rho)\cdot\rho} \qquad \text{(Eq 5)}$$

More assumptions were applied during the development of this attenuation modeling due to inaccessible information of scintillator material and design of CCD and CMOS detectors, and the variation of manufacture process. These assumptions are 1) omitted reflection at the interface between scintillator and faceplate; 2) omitted reflection at the interface between faceplate and CCD/CMOS chip; 3) omitted interaction of incident x-ray with scintillator material (i.e., photoelectric absorption and re-emitted low energy x-ray by Compton scattering); 4) ignored structure distortion and assumed incident x-ray is parallel to fiber axis of faceplate.

4. Discussion of results

4.1 Attenuation curves of core, clad and EMA

The chemical compositions of core, clad and EMA materials used in B7D59-6 and B7D61-6 products are listed in Table 1 and the converted weight fractions of constituent elements are summarized in Table 2.

[redacted]

Proprietary information contact Incom Inc. for data

[redacted]

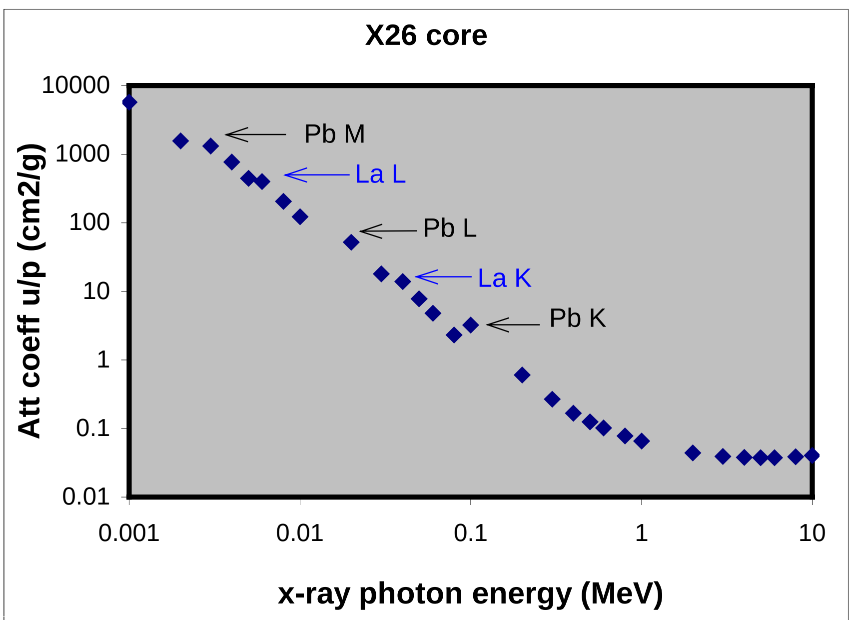

Figure 5- Mass attenuation coefficient of X26 in logarithmic scale

With the weight fraction contribution from each element, the mass attenuation coefficient at photon energy level of 0.1 MeV to 10 MeV is plotted in logarithmic scale in Figure 5 for X26 core material. In general, the attenuation decreases as the photon energy increases. Each kink on attenuation curve represents an absorption edge of certain constituent element. For example, the kink around 0.088 MeV is contributed by K-edge of Pb element. At absorption edge, the attenuation will suddenly increase due to photoelectric effect.

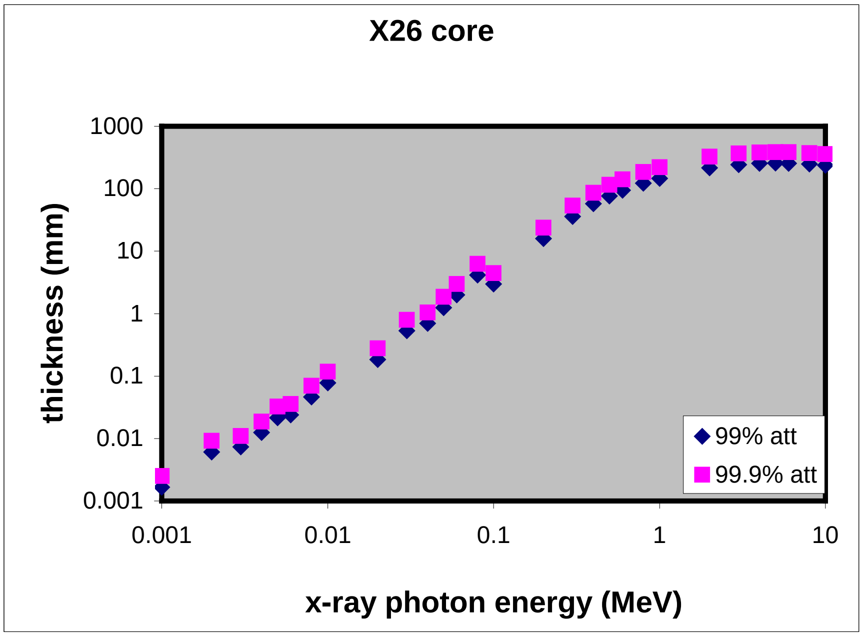

Figure 6 – Required thickness (mm) of X26 core material to attenuate 99% and 99.9% x-ray versus incident photon energy in logarithmic scale.

To better understand the attenuation power of Incom products in imaging applications, let's assume the faceplate is made of core material only. Then the required thickness to attenuate 99% x-ray and 99.9% x-ray is plotted in Figure 6 and the thickness values within diagnostic x-ray energy region summarized in Table 3. The results show that 2 mm of X26 can attenuate 99% and 3 mm can attenuate 99.9% of x-ray if the incident photon energy is at 60 keV. This is an ideal but unrealistic situation, because cladding must be present to make a fiber optic waveguide.

Table 3 - Required thickness (mm) of X26 core material at diagnostic x-ray energy level.

Thickness (mm)

x-ray E (MeV)	0.02	0.03	0.04	0.05	0.06	0.08	0.1
att = 99%	0.2	0.5	0.7	1.2	2.0	4.2	3.0
att = 99.9%	0.3	0.8	1.0	1.9	3.0	6.2	4.5

Similarly, the mass attenuation coefficients of C5 and B7 material are calculated and plotted in Figure 7 and Figure 8 respectively, with absorption edges identified. Comparing these plots to Figure 5, we see that at photon energy level of 0.06 MeV, the x-ray stopping power of cladding is about fifteen times less than that of the core and the x-ray stopping power of EMA is about twenty-five times less than the core. The attenuation differences increase as photon energy increases. Therefore the configuration that favors a higher percentage of core gives better attenuation.

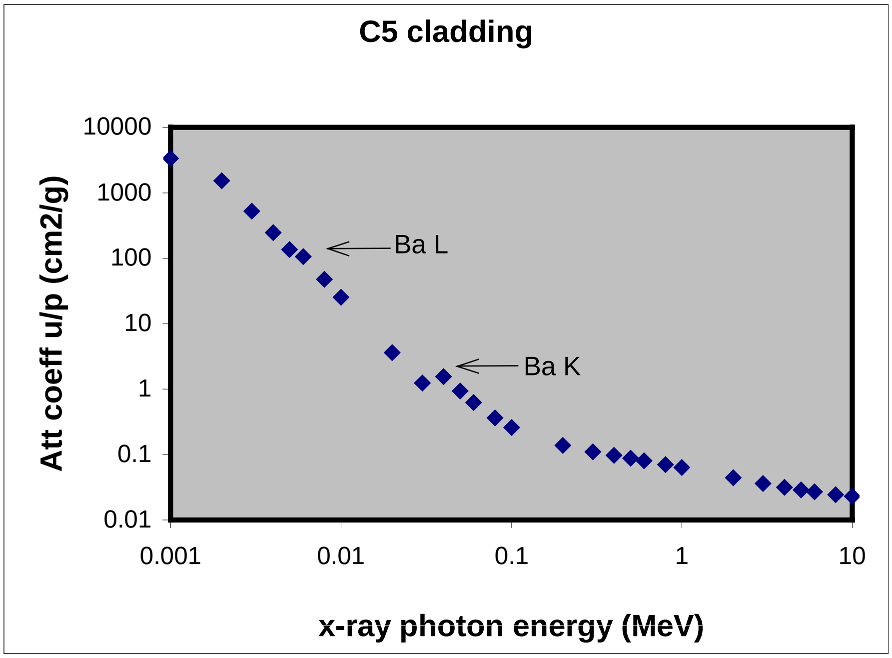

Figure 7 – Mass attenuation coefficient of C5 material as a function of x-ray photon energy in logarithmic scale.

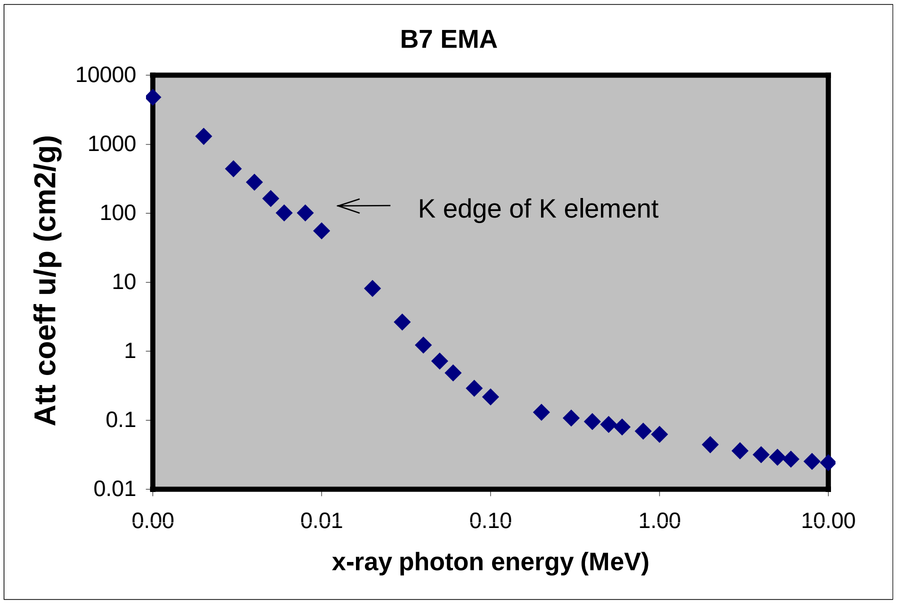

Figure 8 – Mass attenuation coefficient of B7 material as a function of x-ray photon energy in logarithmic scale.

Statistical EMA configurations

Statistical configuration describes a process where EMA are put in replacement of single fiber as illustrated in Figure 9. The three-piece statistical configuration is applied to BIE395-6 and BXE387-6 products. The one-piece statistical configuration is applied to B7D59-6 and B7D61-6 products. The Multi Draw fuses a fiber bundle containing 58 pieces of single fiber and 3 pieces of EMA or 60 pieces of single fiber and 1 piece of EMA. Based on core/clad ratio of each product, the relative area fractions of core, clad and EMA in a unit area in Figure 9 are calculated in a Microsoft Excel template and summarized in Table 4.

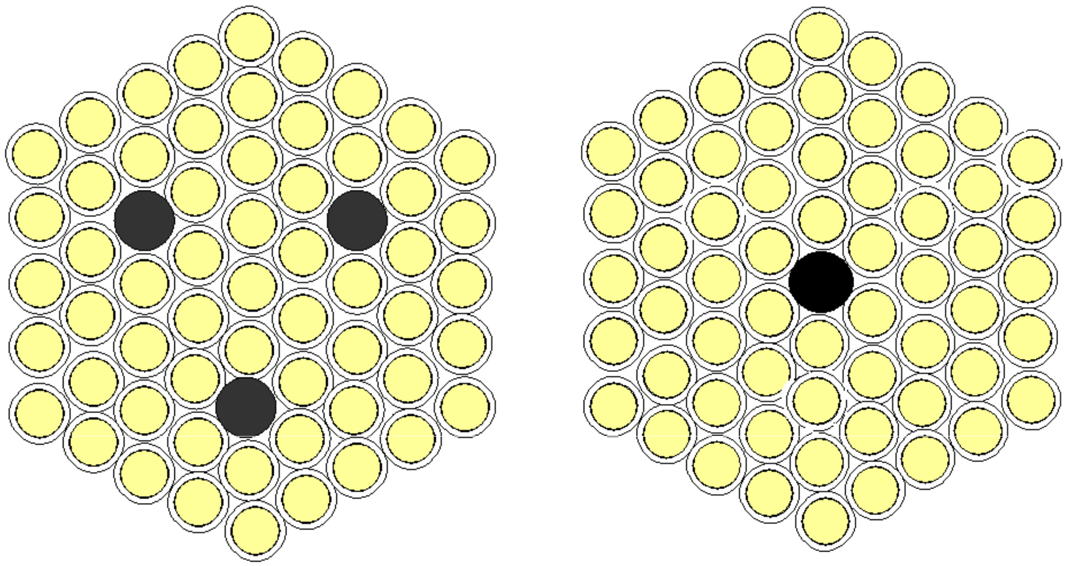

Figure 9 - 3 piece and 1 piece Statistical EMA configurations.

Table 4 - The relative area fraction for products with 3 piece statistical EMA (a) and 1 piece statistical EMA (b).

INCOM Product	BXE387-6	BIE395-6
core/clad ratio	19:1	19:1
core fraction	76.12%	76.12%
clad fraction	18.96%	18.96%
EMA fraction	3.96%	3.96%
EMA clad fraction	0.95%	0.95%

(a)

INCOM Product	B7D59-6	B7D61-6
core/clad ratio	16:1	26:1
core fraction	75.31%	83.25%
clad fraction	23.05%	15.11%
EMA fraction	1.32%	1.32%
EMA clad fraction	0.32%	0.32%

(b)

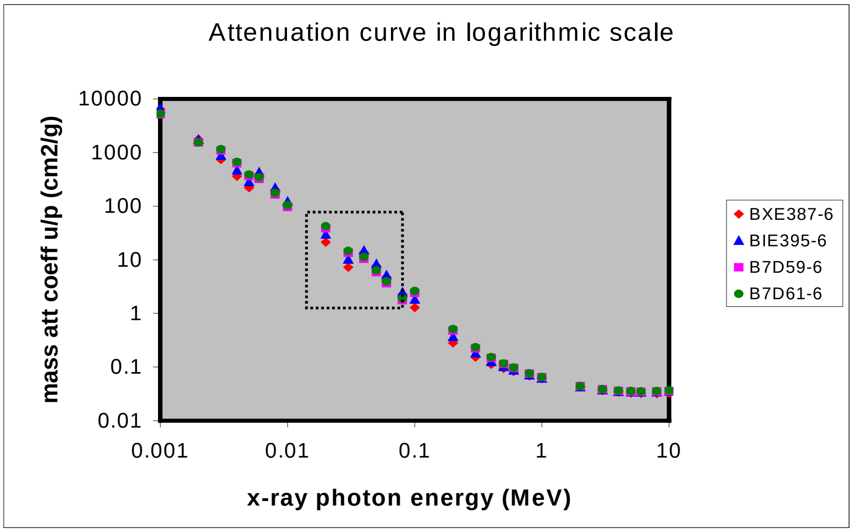

(a)

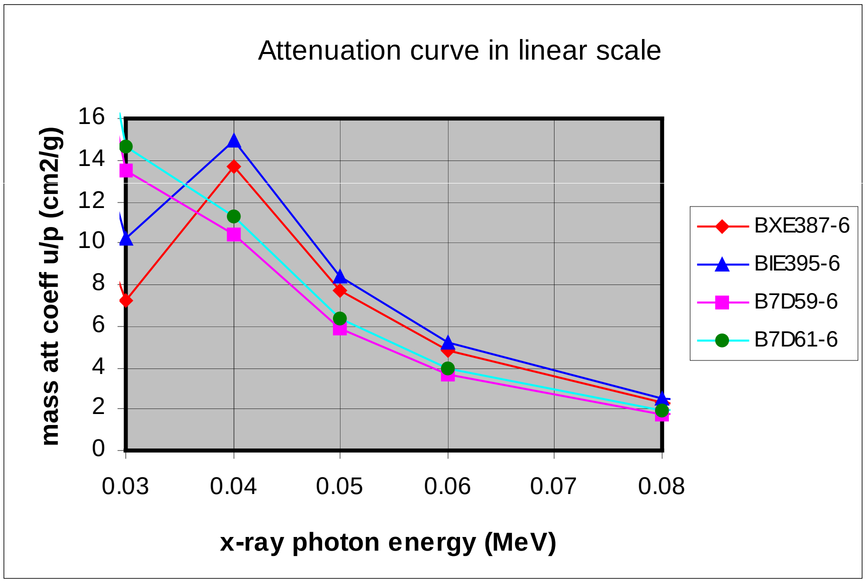

(b)

Figure 10 – (a) Mass attenuation of BXE387-6, BIE395-6, B7D59-6 and B7D61-6 in logarithmic scale. (b) Zoomed in view corresponding to performance of faceplate in diagnostic x-ray region in linear scale.

Table 5 – Mass attenuation coefficient of BXE386, BIE395-6, B7D59-6 and B7D61-6 for x-ray photon energies within the diagnostic x-ray region.

Mass attenuation coefficient u/p (cm2/g)

x-ray (MeV)	0.02	0.03	0.04	0.05	0.06	0.08	0.1
BIE395-6	29.7	10.2	14.9	8.4	5.2	2.5	1.8
BXE387-6	21.4	7.3	13.7	7.7	4.8	2.3	1.3
B7D59-6	13.5	10.4	5.7	3.7	1.8	2.4	0.5
B7D61-6	14.7	11.3	6.3	4.0	1.9	2.6	0.5

From the mass attenuation coefficient of pure core, clad and EMA material and their area fractions, the μ/ρ curve of final product is plotted in Figure 10. From (Eq 5), the faceplate thickness to attenuate 99% of x-ray can be derived (shown in Figure 11 (a)). Again, data within the dashed square is enlarged in Figure 11 (b), which corresponds to diagnostic x-ray of our interest.

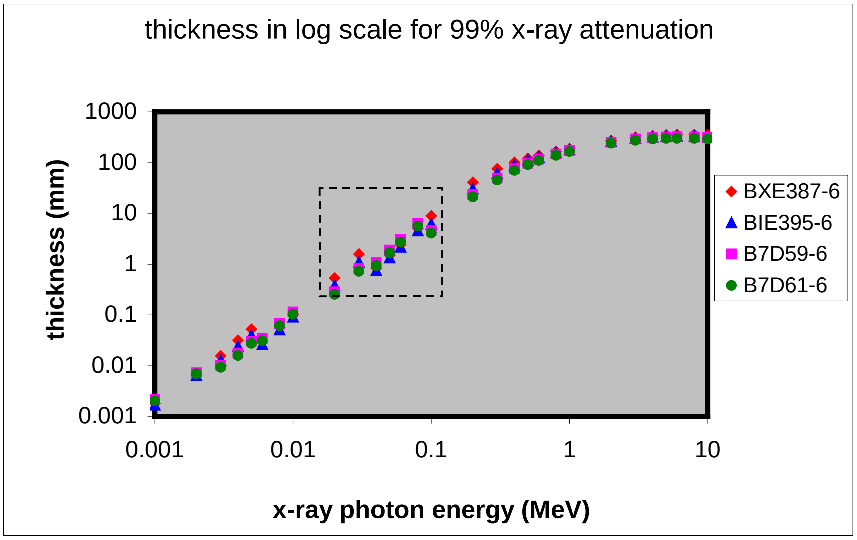

(a)

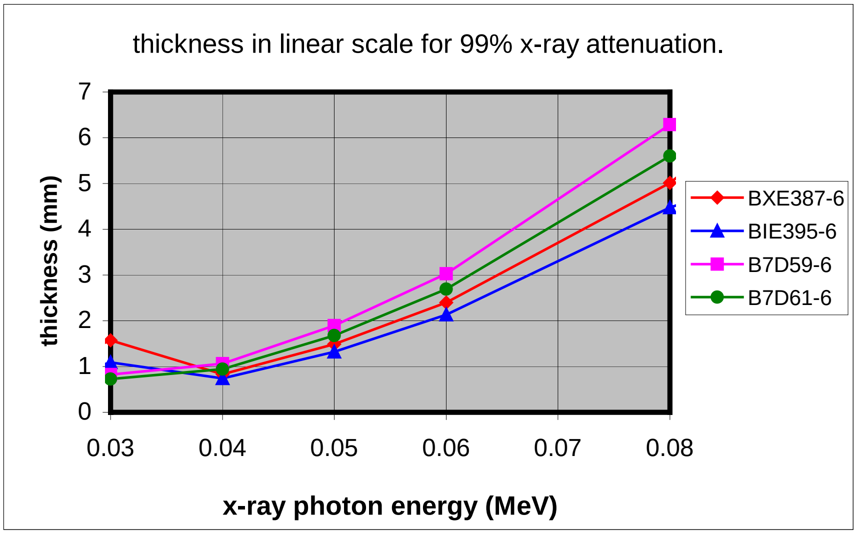

(b)

Figure 11 - (a) The thickness of 99% x-ray attenuation for faceplate with statistical EMA versus photon energy in logarithmic scale. (b) Zoomed in view corresponding to performance of faceplate in diagnostic x-ray region in linear scale.

The thickness value in diagnostic x-ray region from Figure 11(b) is summarized in Table 6. It shows that 1 mm thickness is sufficient to attenuate 99% of x-ray for B7D59-6 and B7D61-6 products if the incident photon energy is no more than 0.03 MeV. For diagnostic X-ray energies of 0.04 MeV and higher, X-14 core compositions consistently achieve 99% attenuation with less glass thickness compared to X26 core materials. For diagnostic X-ray energies of 40 keV or less, X-26 faceplates with X-26 core compositions have greater stopping power for the same thickness. Among the X-14 core compositions, BIE395 compositions perform better than BXE387.

Thickness (mm) to get 99% attenuation

x-ray E (MeV)	0.02	0.03	0.04	0.05	0.06	0.08	0.1
B7D59-6	0.3	0.8	1.1	1.9	3.0	6.3	4.6
B7D61-6	0.3	0.7	0.9	1.7	2.7	5.6	4.1
BXE387-6	0.6	1.6	0.8	1.5	2.4	5.0	8.9
BIE395-6	0.4	1.1	0.7	1.3	2.1	4.5	6.2

Table 6 - The faceplate thickness (mm) of 99% attenuation of diagnostic x-ray (0.02 to 0.1 MeV) for products with statistical EMA.

5. Summary

The x-ray attenuation model for Incom's faceplate product is developed based on mass attenuation coefficient from the database of NIST. The contributions from all constituent elements and geometric configurations with different core/clad ratio are considered.

Result shows that attenuation and required thickness to achieve certain attenuation power are highly photon energy dependent. The lower the photon energy of x-ray, the higher attenuation of faceplate, and less thickness is required. To better market products in different applications, information from customers regarding x-ray photon energy used in a particular application is very important and helpful.

To simplify the calculation, multiple assumptions are applied in the NIST database as well as in the development of this model, which results in a very conservative modeling. For example, scintillator material coated on the surface of faceplate not only absorbs x-ray but also transfers high-energy x-ray to low energy x-ray through Compton scattering process. The accuracy of the model can be evaluated with comparison between modeled attenuation and measured data either from customer or an independent testing organization.

Appendix:

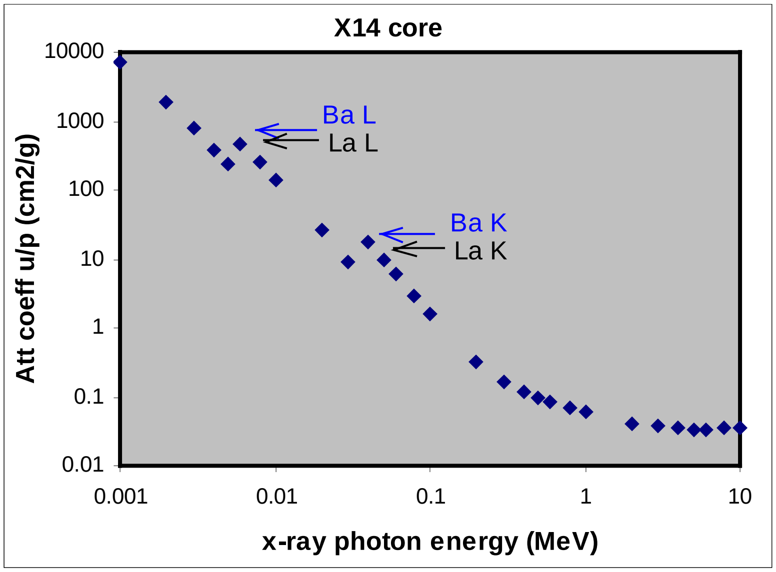

Figure 12 – mass attenuation coefficient of X 14 in logarithmic scale

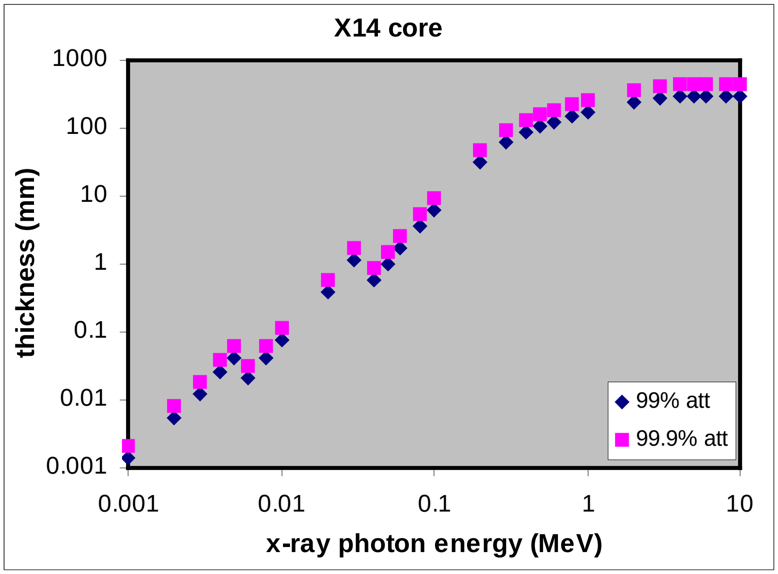

Figure 13 – Required thickness (mm) of X14 core material to attenuate 99% and 99.9% x-ray versus incident photon energy in logarithmic scale.

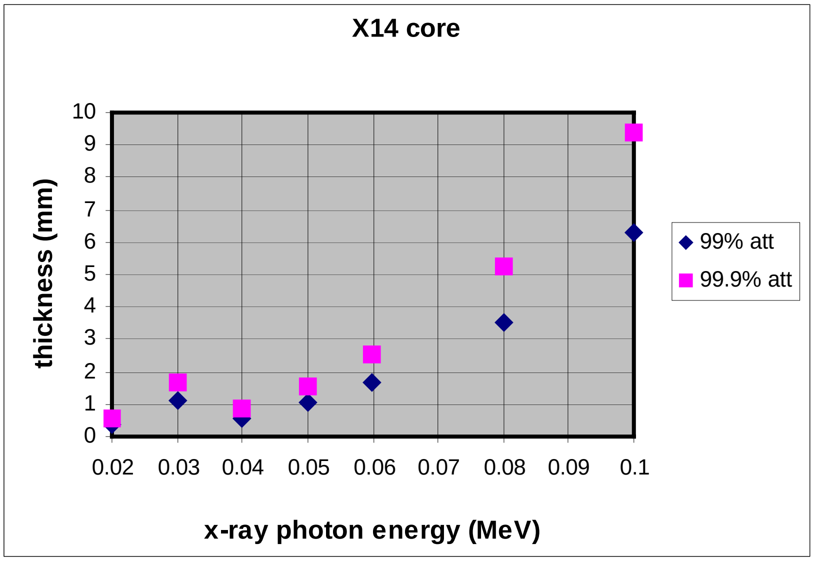

Figure 14 - Required thickness (mm) of X14 core material to attenuate 99% and 99.9% x-ray versus incident photon energy in linear scale, for the diagnostic x-ray region.

Table 7 – Required thickness (mm) of X14 core material at diagnostic x-ray energy level

thickness (mm)

x-ray E (MeV)	0.02	0.03	0.04	0.05	0.06	0.08	0.1
att = 99%	0.4	1.1	0.6	1.0	1.7	3.5	6.3
att = 99.9%	0.6	1.7	0.9	1.5	2.5	5.3	9.4

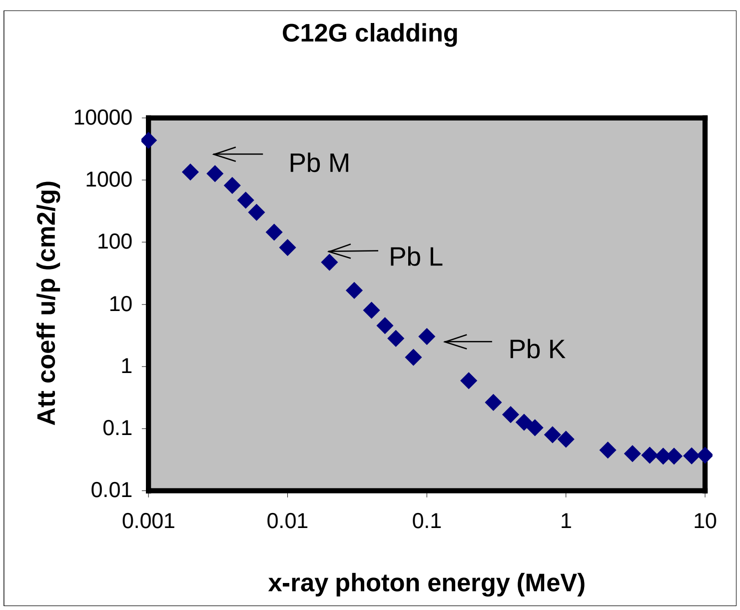

Figure 15 – Mass attenuation coefficient of C12G material as a function of x-ray photon energy in logarithmic scale.

[redacted]

Proprietary information contact Incom Inc. for data

References:

1. J. Wang and T. Blackburn. ‘X-ray image intensifiers for fluoroscopy’. *Radio Graphics*, vol 20, p1471 (2000).
2. ‘The Encyclopedia of Medical Imaging’. Volume I. Copyright Amersham Health.